N.T.

NATIONAL AERONAUTICS AND SPACE ADMINISTRATION

Technical Report 32-1253

Stress Analysis of Solid Propellant Rocket Motors

F. A. Akyuz

E. Heer

JET PROPULSION LABORATORY

CALIFORNIA INSTITUTE OF TECHNOLOGY

PASADENA, CALIFORNIA

July 1, 1968

NATIONAL AERONAUTICS AND SPACE ADMINISTRATION

Technical Report 32-1253

Stress Analysis of Solid Propellant Rocket Motors

F. A. Akyuz
E. Heer

Approved by:

W. H. Gaynan

for M. E. Alper, *Manager*
Applied Mechanics Section

JET PROPULSION LABORATORY
CALIFORNIA INSTITUTE OF TECHNOLOGY
PASADENA, CALIFORNIA

July 1, 1968

TECHNICAL REPORT 32-1253

Prepared Under Contract No. NAS 7-100
National Aeronautics & Space Administration

Contents

Figures

Contents (contd)

Figures (contd)

Abstract

A brief description of problems in the stress analysis of solid propellant rocket motors is given with a short review of related recent literature. The general linear viscoelastic and elastic problem, some possible means of solution, and the hypotheses and assumptions involved are discussed. A brief account of the computer program ELAS for elastic analyses is given. Solutions of typical two- and three-dimensional problems are presented and compared with those obtained by others. The effect of Poisson's ratio close to 0.5 on the computed results has been evaluated and is discussed. Possible future developments of the numerical methods of analysis in connection with available theories and analytical works are outlined.

Stress Analysis of Solid Propellant Rocket Motors

I. Introduction

Problems in the aerospace industry are often associated with the structural integrity of solid propellant grains. Although research in this area is beginning to be used effectively, further work is required to establish stress analysis as a reliable engineering tool in the design of structurally sound propellant grains consisting of nonlinear viscoelastic materials with mechanical properties that are highly sensitive to temperature.

The ultimate goal of solid propellant stress analysis is to determine deformation and stress histories in propellants and casings of rocket motors and to predict internal geometrical integrity, fracture, and failure. This requires a thorough understanding of solid propellant material behavior under various environmental conditions, especially temperature changes. It also requires a continuing systematic assessment so that realistic constitutive relations (stress–strain relations) can be considered and incorporated in the stress analysis. In addition, it requires capabilities in advanced numerical techniques suitable to determine stresses in complex solid propellant grain configurations. Needless to say, all these areas require much additional work beyond the present state of the art in order to be able to analyze, with confidence, currently used solid propellant motors. Purely analytical techniques are applicable only to some of the most simple cases imaginable, and we must, therefore, resort to other approaches that are believed to be more suitable for these problems.

The upsurge of the finite element technique in structural technology during the last few years has given a tool to the stress analyst which provides the flexibility as well as the versatility necessary for the analysis of structural problems with complex boundary conditions, complex loading conditions, and complex configurations. A vast literature exists about the finite element technique and its application, mainly to elastic and plastic static problems and to some steady state dynamic problems (e.g., Refs. 1 and 2). However, the extension of this technique to viscoelastic problems has been accomplished only in a few relatively simple cases (e.g., Ref. 3).

In the present report we first review some recent literature in solid propellant thermoviscoelasticity in the light of recent developments and with a view to a possible finite element approach. We then discuss some of the main ingredients of stress analysis and some of the underlying assumptions related to the constitutive equations,

geometrical constraints, boundary conditions, and failure criteria. Some methods of stress analysis, in particular the finite element method, are reviewed in some detail. Specifically, a finite element computer program for static linear elastic problems, called ELAS, is discussed with respect to its possible extension to handle linear thermoviscoelastic problems. Finally, stress analysis results for various solid propellant motors are computed with ELAS and compared with similar analyses obtained by others using different analysis techniques. Additional results for two- and three-dimensional stress analyses and for Poisson's ratio close to 0.5 are given.

II. Review of Some Recent Literature

The analysis of solid propellant grains has occupied the attention of engineers for a number of years, and a considerable amount of literature, directly or indirectly related to this problem, has been generated. For instance, Ref. 4 refers to 52 relevant publications.

In a series of publications (Refs. 5–7), Biot developed a linear theory of thermoviscoelasticity based on the thermodynamics of irreversible processes using Lagrangian methods of generalized coordinates.

Shapery extended Biot's theory to a special class of nonlinear behavior in Ref. 8 and demonstrated correlation with experimental results for unfilled and filled polymers. In Ref. 9, Shapery modified Biot's theory by considering explicit temperature dependence of material properties and the inclusion of the time–temperature superposition principle for treating media with temperature-dependent viscosity. In Ref. 10, the linear, nonisothermal constitutive equations and energy equation of Ref. 9 were extended to nonlinear materials with transient, nonuniform temperatures; also, the temperature dependence of viscosity was introduced through the familiar assumption of thermorheologically simple behavior, which is extensively discussed in Refs. 11 and 12.

In many linear problems, the elastic–viscoelastic correspondence principle of Alfrey (Ref. 13) is useful in obtaining solutions to viscoelastic problems. In particular, for solid propellant grains, as pointed out by Fitzgerald (Ref. 4), the elastic–viscoelastic correspondence principle is useful to obtain solutions to isothermal stress problems, isochoric pressurization problems, and certain gravitational slump problems. Provided the physical properties of the material are assumed to be independent of temperature, an elementary extension of the correspondence principle ordinarily also permits a systematic reduction of viscoelastic problems with transient temperature fields to associated thermoelastic problems (Ref. 14).

Muki and Sternberg (Ref. 15) dealt with the analysis of transient thermal stresses in linear viscoelastic solids with temperature-dependent material properties, where the underlying constitutive law rests on the temperature–time equivalence hypothesis, i.e., for thermorheologically simple materials. Even though there seems to be no comprehensive method of solving this system of equations with time-dependent properties, Muki and Sternberg obtained the thermal stress field during transient temperature conditions in two particular cases for a plate and for polar symmetry.

Because the material properties of solid propellants are extremely temperature-sensitive, it is not possible, in general, to utilize the correspondence principle for their analysis if the thermal field is time-dependent. The correspondence principle is usually inapplicable also if the boundary of the region under consideration is moving, i.e., if the motion of the interior surface of the solid propellant grain during burn must be accounted for in the analysis. Before applying the correspondence principle in the analysis of solid propellants, a thorough evaluation of its applicability should, therefore, be made.

In employing numerical techniques for the stress analysis of solid propellants, the correspondence principle can be applied with advantage only to isothermal and isochoric problems where synchronous separation of the variables is evident. A comprehensive review of such numerical methods is given by Parr in Ref. 16.

To date, it seems that the only paper published in the open literature which directly applies the finite element technique to the analysis of linear thermoviscoelastic problems, without utilizing the correspondence principle, is by Taylor and Chang, Ref. 3. They considered specifically axisymmetric and point-symmetric boundary value problems using the virtual displacement principle and employing a step-forward integration scheme, in time, to solve the set of equations under the assumption of thermorheologically simple behavior. The maximum number of equations handled was 20, and, because of the involved symmetries, only one dimension (the radial) had to be considered. The amount of computational effort, therefore, did not seem to pose great problems. However, Taylor and Chang indicated that the numerical integrations of the simultaneous integral equations are time-consuming and that some improvements are necessary before large arrays of elements can be analyzed.

Because of the above-described developments and the rapid increase in computational operations with the inclusion of additional spatial dimensions, the additional time dimension, and additional finite elements, it did not appear economically feasible to modify or to extend existing general computer programs such as SAMIS (Ref. 17) to include analysis capabilities for the thermoviscoelastic response of propellant grains. Motivated by these considerations, Utku and Akyuz developed a computer program (ELAS, Ref. 18) that is capable of handling static elastic problems with the appropriate speed and efficiency to make it suitable for extension and inclusion of thermoviscoelastic analysis capabilities. In this report, ELAS has been used for the computation of displacements and stresses in solid propellants under the assumption of linear elastic behavior only. Work to extend ELAS (Ref. 18) to include viscoelastic behavior also is presently in progress.

III. Components of Stress Analysis and General Assumptions

In this section, the components of solid propellant stress analysis are delineated and defined as they are generally used throughout the solid propellant industry.

A. Geometry

The geometry of solid propellant grains is determined at the exterior surface by the rocket casing and at the interior by the grain cavity. While the exterior boundary can be considered constant, i.e., independent of time, certain equilibrium and compatibility conditions have to be satisfied at the propellant–casing interface. The interior boundary, on the other hand, changes its position appreciably during burn. Thus, the analysis must deal with a time-dependent, moving boundary. However, since the most critical problems of solid propellant analysis fortunately occur before burn, in this study we shall also assume a constant, time-independent interior boundary shape.

While the exterior surface of the solid propellant frequently has a relatively simple configuration such as a sphere, a cylinder, or a sphere–cylinder combination, the interior cavity is very often quite irregular in design, showing, e.g., star-like configurations with slots, recesses, etc. Such configurations are particularly bothersome in a purely analytical formulation, where it is almost mandatory that the shape of the boundary be representable by a coordinate surface. With the use of the finite element method, however, the shape of the boundary has only slight significance. Special assumptions about the geometry of the boundary are therefore not necessary.

For the sake of generality and compactness, the equations will be developed as far as possible utilizing the now-familiar tensor calculus in general curvilinear coordinates, as presented in Ref. 19. Definitions of metric tensors g_{ij} and g^{ij} and associated tensor manipulations are given in the same reference.

B. Loading

The loadings of solid propellants for rocket motors can result from externally applied forces at the boundary; body forces, such as gravity forces, centrifugal forces and acceleration forces; and forces due to temperature changes.

The external forces are mainly due to given internal pressures and shear stresses at the cavity boundary and to differential expansions of casing and grain under temperature changes. Body forces as a result of the earth's gravitational field may be of long duration during storage and may cause creep deformations leading to the so-called gravitational slump. Centrifugal forces occurring, e.g., during spin-up, and acceleration forces resulting, e.g., from impact loadings, vibrations, and launch are usually of short duration.

In determining thermal stresses, it may sometimes be necessary, for very high strain rates, to consider the effect of the strain field on the thermal field. We shall assume here the applicability of the "uncoupled theory," where the thermal field can be determined independently of the mechanical field, but where the effects of thermal changes in the constitutive equations of the material are considered. The thermal field in the solid propellant is assumed to be given as a function of location and time.

C. Boundary and Initial Conditions

The conditions at the boundary of the solid propellant can be given by prescribed surface forces mentioned above, by prescribed displacements, or by interface conditions where the unknown stresses and/or displacements are determined using the appropriate equilibrium and compatibility conditions.

At points on the bounding surface where stress conditions are prescribed, it is required that the internal stresses τ^{ij}, evaluated at the surface S, balance the externally applied forces. If $\mathbf{n}$ is the unit normal vector to the surface at the point under consideration (Fig. 1) and

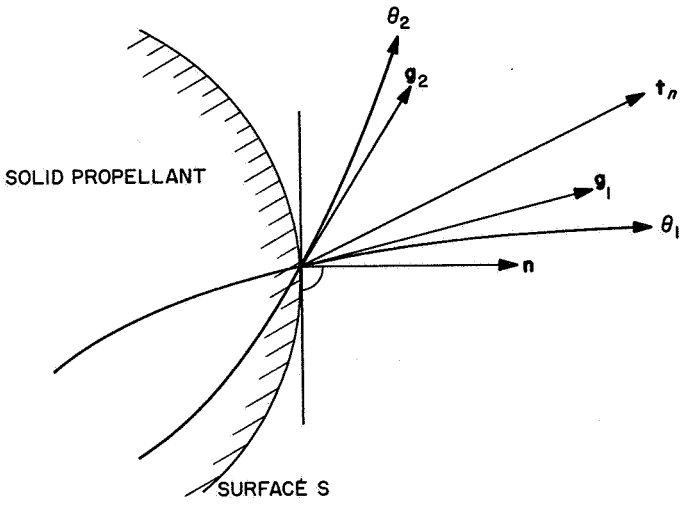

Fig. 1. Boundary point showing in two dimensions the curvilinear coordinate lines θ_1 and θ_2, the unit normal vector n, the covariant base vectors $\mathbf{g}_1$ and $\mathbf{g}_2$, and the externally applied force vector $\mathbf{t}_n$

the $\mathbf{g}_j$ are the covariant base vectors referred to an arbitrary curvilinear coordinate system, then the externally prescribed force vector $\mathbf{t}_n$ at this point requires that

$$n_i \tau^{ij} \mathbf{g}_j|^S = \mathbf{t}_n \tag{1}$$

At points on the boundary where the externally prescribed displacement vector is $\mathbf{u}^{(E)}$, it is required that the displacement vector evaluated at the boundary satisfy

$$\mathbf{u}|^S = \mathbf{u}^{(E)} \tag{2}$$

The initial conditions will be specified so that all field quantities, displacements, velocities, stresses, strains, etc., vanish for $t < 0$.

D. Material Properties

The support for solid propellant grains is sometimes provided not only by the motor casing but also by internally placed reinforcing wires or fibers. Solid propellant grains therefore frequently exhibit anisotropic properties, which are characteristic of composite materials. Although the structural response of the grain material is often nonlinear, we assume linear behavior as a first step toward the analysis of such general materials. We assume further that the material behaves in a thermorheologically simple way, showing, for changes of temperature, a pure shift in the creep functions, relaxation moduli, and other characteristic functions of the material, when these are plotted against the logarithm of time.

Let $E^{ijkl}(t)$ be the general anisotropic relaxation moduli of the fourth-order material property tensor, which has the following symmetry properties:

$$E^{ijkl} = E^{jikl} = E^{ijlk} = E^{klij} \tag{3}$$

and therefore has 21 independent components.

To express thermorheologically simple behavior analytically (Refs. 11 and 12) we define a "reduced time" by

$$\xi(\mathbf{x}, t) = \int_0^t \frac{dt'}{a_T[T(\mathbf{x}, t')]} \tag{4}$$

where a_T is the time shift function and T is the temperature. For each relaxation modulus the following relation holds:

$$E_T^{ijkl}(t) = E_{T_0}^{ijkl}(\xi) \tag{5}$$

Equation (5) states that the relaxation moduli at an arbitrary temperature T corresponding to time t are expressed by their behavior at the reference temperature T_0 related to the new "reduced" time scale ξ.

The time shift function a_T in Eq. (4) is an experimentally determined function (Ref. 20) of temperature T only; its dependence on position x and time t is implicit through T and is well described by the Williams–Landel–Ferry (WLF) equation,

$$a_T = \exp\left[-\frac{C_1(T - T_g)}{C_2 + (T - T_g)}\right] \tag{6}$$

where T_g is the glass transition temperature of the polymer and C_1 and C_2 are constants.

The difference between the local instantaneous temperature $T(\mathbf{x}, t)$ and the conveniently selected reference temperature T_0, for which a zero stress and deformation state is assumed, is the thermal field history designated by

$$\theta(\mathbf{x}, t) = T(\mathbf{x}, t) - T_0 \tag{7}$$

The linear coefficients of thermal expansion α'_{kl} represent a second-order symmetric tensor with six independent thermal expansion coefficients in the general case.

The coefficients $\alpha'_{kl}(T')$ usually are functions of temperature. We then define the average coefficient $\alpha_{kl}(T)$ by

$$\alpha_{kl}(T) = \frac{1}{\theta}\int_{T_0}^{T} \alpha'_{kl}(T')\,dT' \tag{8}$$

With the strain tensor γ_{kl}, the general linear viscoelastic constitutive equations can now be written in the general form of hereditary integrals as

$$\tau^{ij}(\mathbf{x},t) = \int_{-\infty}^{t} E^{ijkl}[\xi(\mathbf{x},t) - \xi'(\mathbf{x},t')]\frac{\partial}{\partial t'}[\gamma_{kl}(\mathbf{x},t') - \alpha_{kl}(\mathbf{x},t')\,\theta(\mathbf{x},t')]\,dt' \tag{9}$$

where[1] the argument $\xi(\mathbf{x},t) - \xi'(\mathbf{x},t')$ is obtained using Eq. (4) and is in general a complicated nonlinear function of time. Because of this nonlinearity it is not possible to remove the time dependence by taking Laplace transforms of Eq. (9), i.e., the dependence on time of the temperature; and hence the shift function makes it, in general, impossible to invoke the correspondence principle.

In terms of mixed tensors, Eq. (9) becomes

$$\tau^i_j(\mathbf{x},t) = \int_{-\infty}^{t} E^{ik}_{jl}(\xi - \xi')\frac{\partial}{\partial t'}(\gamma^l_k - \alpha^l_k\theta)\,dt' \tag{10}$$

For isotropic material the mixed stress and deformation tensors can be split into dilatational and deviatoric parts. With the Kronecker delta δ^i_j, the deviatoric stress tensor s^i_j and the deviatoric strain tensor e^l_k we obtain

$$\tau^i_j = \frac{1}{3}\delta^i_j\tau^k_k + s^i_j \tag{11}$$

$$\gamma^l_k = \frac{1}{3}\delta^l_k\gamma^m_m + e^l_k \tag{12}$$

The mixed material tensor for the isotropic case becomes, with shear modulus $G(\xi)$ and bulk modulus $K(\xi)$,

$$E^{ik}_{jl}(\xi) = G(\xi)\left\{g^{ik}g_{jl} + \delta^i_l\delta^k_j + \left[\frac{K(\xi)}{G(\xi)} - \frac{2}{3}\right]\delta^i_j\delta^k_l\right\} \tag{13}$$

while the tensor of the average thermal expansion coefficients becomes

$$\alpha^l_k = \delta^l_k\alpha \tag{14}$$

[1]The usual summation convention is used.

Substituting Eqs. (11)–(13) in Eq. (10) and multiplying yields two independent constitutive equations as follows:

(1) The dilatational equation,

$$\tau^k_k(\mathbf{x},t) = 3\int_{-\infty}^{t} K(\xi - \xi')\frac{\partial}{\partial t'}(\gamma^k_k - 3\alpha\theta)\,dt' \tag{15}$$

(2) The deviatoric equation,

$$s^i_j(\mathbf{x},t) = 2\int_{-\infty}^{t} G(\xi - \xi')\frac{\partial}{\partial t'}e^i_j\,dt' \tag{16}$$

For the isotropic elastic material, we have

$$\tau^k_k = 3K(\gamma^k_k - 3\alpha\theta) \tag{17}$$

$$s^i_j = 2G\,e^i_j \tag{18}$$

or

$$\tau^i_j = 2G\left(\gamma^i_j - \frac{\nu}{1-2\nu}\delta^i_j\gamma^k_k\right) \tag{19}$$

where ν is Poisson's ratio.

Frequently it can be assumed that in isotropic material only the deviatoric part responds viscoelastically (Eq. 16), while the dilatational part responds elastically (Eq. 17). A further assumption that is often justified for viscoelastic analyses is that the material is incompressible. In such cases, only Eq. (16) or Eq. (18) is used for viscoelastic or elastic analysis, respectively.

Many solid propellants have Poisson's ratio close to 0.5, i.e., they behave very nearly incompressibly. The assumption of incompressibility would, therefore, introduce only

small errors. However, in using the finite element technique, the numerical difficulties encountered by this assumption seem to outweigh by far the analytical simplifications frequently realized in purely analytical work. In this report we shall, therefore, always assume that the material is at least slightly compressible, and we shall show for elastic materials, utilizing the finite element technique, the behavior of some numerical results close to incompressibility.

E. Failure Criteria

The structural systems of solid propellant motors consist of a relatively weak propellant grain of elastomeric or polymeric binder loaded with a high percentage of granular fuel and metal oxidizer, surrounded by a metallic or composite material case which provides the essential structural resistance against the forces due to pressurization and thermal strains. Because of pressurization and thermal changes, we encounter large strains near the burning surface and near the interface between grain and casing, owing to large thermal expansion differences and large differences in the relaxation moduli of the adjacent materials. If the strength of the grain material at these strain levels is inadequate, grain failure will be caused by cracking or by interface failure between grain and casing. Although the cracking and interface failures do not seriously impair the structural strength of the motor, they can seriously reduce its operational capability.

Failure analysis of the motor has, therefore, the twofold requirement of deformation and strength analysis of the case and deformation and strength analysis of the grain. The former analysis is mainly concerned with structural integrity, while the latter is mainly concerned with operational integrity. The case analysis can be handled reasonably well with present structural mechanics technology, while the grain analysis requires extensive fundamental work at the research level for the development of reliable failure criteria. This need exists because the filler–binder compound can be considered as a reasonably continuous medium only at relatively small strains. It loses its continuity at strains that are considerably below those at which cracks actually start to propagate throughout the medium. Unfortunately for the application of continuum mechanical theory to grain analysis, particularly close to failure, the level of maximum operational strains due to pressurization and to thermal cycles is within this intermediate quasi-discontinuous range of behavior. Hence, we are dealing here with a quasi-static time-dependent accumulation of breakdown of the material until catastrophic fracture occurs. This is an irreversible kinetic process that starts with imbedded minute disturbances such as flaws, particles, etc., which randomly permeate the material, and ends with the uncontrollable propagation of at least one crack. Thus in a "homogeneous" grain material there is, at each point, the potential for generating a multitude of cracks for a given excitation. Often many cracks are initiated very early after loading; however, the density of continuously growing cracks seems to decrease sharply with the passage of time, and rupture is usually observed to be the result of the rapid propagation of only one or two cracks, while the remaining potential cracks remain dormant. For this reason, fracture theories employing the expedient concept of a single critical flaw are often quite successful in practice. To a large extent, it is also for this reason that in failure analysis using the concepts of probability theory, we employ the theory of extreme value statistics, in which we ask for the probability distributions of extreme flaw sizes.

Knowing the extreme flaw size distributions in the material by assumption or from experiment, and having computed the internal stress state histories in the solid propellant grain, we must establish a causal relationship between (1) the state of stress history at a point and (2) the accumulation of breakdown, i.e., the increase of flaw size until it reaches its critical value at rupture. We can then predict the probability of failure or the reliability of a solid propellant grain at each point and as a whole.

While comparatively much work has been done in the area of determining bulk stress state histories, as discussed in the previous section, very little is available in the area of fracture in viscoelastic materials subjected to multiaxial stress states. However, the works that have been published in this area and closely related areas, e.g., Refs. 21 and 22, show that promising steps can be, and are being, taken toward the solution of these problems.

IV. Methods of Analysis

This section gives the analytical background and develops some basic equations for the finite element technique as applied to linear viscoelastic materials. In this discussion we start with the general case of anisotropic temperature-dependent materials and successively reduce the equations to the particular case of elastic materials. Using Laplace transform techniques, it is shown for what

cases and under what conditions the solutions of the corresponding elastic problem are applicable. We then discuss in some detail the capabilities of the ELAS program, with specific reference to its applicability to solid propellant stress analyses.

A. Analytical Background

The general field equations of linear thermoviscoelasticity are:

(1) Equilibrium equations (neglecting acceleration forces),

$$\tau^{ij}|_i + f^j = 0 \tag{20}$$

(2) Strain-displacement equations,

$$\gamma_{ij} = \frac{1}{2}(u_i|_j + u_j|_i) \tag{21}$$

(3) Constitutive equations,

$$\tau^{ij} = \int_{-\infty}^{t} E^{ijkl}(\xi - \xi')\frac{\partial}{\partial t'}(\gamma_{kl} - \alpha_{kl}\theta)\,dt' \tag{22}$$

where ξ, α_{kl}, and θ are as defined in Section III, and where f^j is the contravariant component of the body force per unit volume.

The complete statement of the problem requires the specification of the boundary conditions and initial conditions as given in Section III.

The virtual work is obtained from Eq. (20). Multiplying through by $\mathbf{g}_j$, recognizing that

$$\tau^{ij}|_i\,\mathbf{g}_j = \frac{1}{g^{1/2}}(g^{1/2}\tau^{ij}\,\mathbf{g}_j),_i$$

(Ref. 19), multiplying by the virtual displacement of $\delta\mathbf{u}$, and integrating over the volume V under consideration, yields

$$\int_V \left[\frac{1}{g^{1/2}}(g^{1/2}\tau^{ij}\,\mathbf{g}_j),_i + \mathbf{f}\right]\cdot\delta\mathbf{u}\,dV = 0 \tag{23}$$

By the usual procedure of applying Gauss' theorem and converting the first term in Eq. (23) (Ref. 19) to a volume and surface integral, we obtain the principle of virtual work,

$$\int_V \tau^{ij}\,\delta\gamma_{ji}\,dV = \int_V \mathbf{f}\cdot\delta\mathbf{u}\,dV + \int_S \mathbf{t}_n\cdot\delta\mathbf{u}^{(E)}\,dS \tag{24}$$

which states that the work done by the internal stresses τ^{ij}, when going through the virtual strains $\delta\gamma_{ji}$, is equal to the work done by the body forces $\mathbf{f}$ and by the forces $\mathbf{t}_n$ at the surface S with surface unit normal $\mathbf{n}$ when going through the virtual displacements $\delta\mathbf{u}$.

Equation (24), together with Eqs. (21) and (22) and the assumptions of Section III, is necessary to formulate the finite element approach to viscoelastic problems.

B. Finite Element Method

A general approach to the solution of elasticity problems and other continuum problems is provided by the finite element method, which has been used extensively during the last decade to solve problems of linear elasticity. As mentioned above, very few papers treating other than linear elastic or plastic problems have been published.

The finite element method, based on the essential ideas of the well-known approximation techniques of the Ritz procedure of assuming a displacement field with a sufficient number of undetermined parameters, is versatile enough, within the limitations of finite elements, to accommodate complex configurations, boundary conditions, loadings, and material properties. In the limit, as the finite element sizes tend to zero as their number for the same domain increases indefinitely, it is expected that the results approach their actual true values, although this has not yet been proved for other than simple cases with assumed linear deflection functions.

In the finite element method, the domain for which displacements and/or stresses are to be computed is subdivided into suitably small subdomains called elements, which are connected to each other at the nodal points. The purpose is to obtain a Ritz-type approximate solution for each element in terms of the unknown displacements at the nodal points, and then, by imposing the equilibrium at the nodal points to establish the set of equations to be solved in order to yield the solution for the entire domain.

In the following brief development of the finite element method, we start with the assumption of a rheologically simple material. Without loss of physically and procedurally meaningful generality, we refer to a rectangular cartesian coordinate system in which covariant derivatives become partial derivatives and in which no difference exists among covariant, mixed, and contravariant tensor components.

Substituting Eq. (22) in Eq. (24) gives

$$\int_V \delta\gamma_{ji} \int_{-\infty}^{t} E_{ijkl} \frac{\partial}{\partial t'} (\gamma_{kl} - \theta\alpha_{kl})\, dt'\, dV = \int_V \delta\mathbf{u} \cdot \mathbf{f}\, dV + \int_S \delta\mathbf{u}^{(E)} \cdot \mathbf{t}_n\, dS \tag{25}$$

We now subdivide the entire body under consideration into volume elements (finite elements) which are connected to each other at the nodal points. In the Ith volume element with volume V_I, we assume a displacement field of the following form:

$$\mathbf{u}(\mathbf{x}, t) = \sum_i \boldsymbol{\phi}_{(i)}(\mathbf{x})\, q_{(i)}(t) \tag{26}$$

where the $\boldsymbol{\phi}_{(i)}$ are assumed functions of position, the $q_{(i)}(t)$ are the unknown time-dependent generalized coordinates, and the subscripts in parentheses indicate that these quantities are not vector components. The spatial functions $\boldsymbol{\phi}_{(i)}(\mathbf{x})$ are to be chosen so that compatibility at the boundary between adjacent elements is preserved. There are as many generalized coordinates associated with an element as nodal displacement degrees of freedom. Using matrix notation, Eq. (26) can be written in the form

$$\{\mathbf{u}\} = [\boldsymbol{\phi}]\,\{\mathbf{q}\} \tag{27}$$

where { } and [ ] indicate, respectively, column and rectangular matrices.

The nodal displacements are equal in number to the generalized coordinates and are

$$\{\mathbf{U}\} = [\boldsymbol{\Phi}]\,\{\mathbf{q}\} \tag{28}$$

in which the matrix $[\boldsymbol{\Phi}]$ is formed by successively introducing each nodal point coordinate into Eq. (27). The matrix elements in Eq. (28) are, thus, not functions of $\mathbf{x}$. We solve for the generalized coordinates by

$$\{\mathbf{q}\} = [\boldsymbol{\Phi}^{-1}]\,\{\mathbf{U}\} \tag{29}$$

Using Eqs. (21) and (26), we are able to form a column matrix of the strain components $\{\boldsymbol{\gamma}\}$ in terms of the generalized coordinates

$$\{\gamma\} = [\psi]\,\{\mathbf{q}\} \tag{30}$$

where the elements of the rectangular matrix $[\psi]$ are functions of $\mathbf{x}$ involving $\boldsymbol{\phi}_{(i)}$ and their derivatives. Using Eq. (29) and the transpose law for matrix products, the transpose of the column matrix of the variation of the strain components in Eq. (25) becomes, in matrix notation,

$$\{\delta\gamma\}^{\mathrm{T}} = \{\delta\mathbf{U}\}^{\mathrm{T}}\,[\boldsymbol{\Phi}^{-1}]^{\mathrm{T}}\,[\psi]^{\mathrm{T}} \tag{31}$$

If $[\mathbf{E}]$ is the matrix of the material property functions E_{ijkl}, if $\{\boldsymbol{\alpha}\}$ is the column matrix of the mean thermal expansion coefficients α_{kl}, and if $\{\mathbf{t}_n\}$ is the column matrix of the nodal force components, then, from Eq. (25) with Eqs. (27), (29), (30), and (31), we obtain

$$\begin{aligned}\{\mathbf{t}_n\} = &\int_{V_I} [\boldsymbol{\Phi}^{-1}]^{\mathrm{T}}\,[\psi]^{\mathrm{T}} \int_{-\infty}^{t} [\mathbf{E}]\,[\psi]\,[\boldsymbol{\Phi}^{-1}]\,\frac{\partial}{\partial t'}\{\mathbf{U}\}\, dt'\, dV_I \\ &- \int_{V_I} [\boldsymbol{\Phi}^{-1}]^{\mathrm{T}}\,[\psi]^{\mathrm{T}} \int_{-\infty}^{t} [\mathbf{E}]\,\frac{\partial}{\partial t'}\{\theta\boldsymbol{\alpha}\}\, dt'\, dV_I \\ &- \int_{V_I} [\boldsymbol{\Phi}^{-1}]^{\mathrm{T}}\,[\boldsymbol{\phi}]^{\mathrm{T}}\,\{\mathbf{f}\}\, dV_I\end{aligned} \tag{32}$$

In order to define the problem completely, we must specify two types of connecting conditions at each nodal point: the equilibrium conditions and the compatibility conditions. The equilbrium conditions specify that at each nodal point the sum of all nodal forces $\mathbf{t}_n$ of the adjacent elements and of the externally applied forces $\mathbf{F}$ vanishes. The compatibility conditions require that at each nodal point the adjacent elements undergo the same displacement. Substituting Eq. (32) in the equilibrium conditions and utilizing the compatibility conditions, we obtain a set of linear integral equations with the nodal displacements $\{\mathbf{U}\}$ as unknown functions and the externally applied forces $\mathbf{F}$ as inputs. In addition, we have to impose boundary conditions at the boundary nodes and initial conditions at all nodes as indicated in Section III.

The matrix elements E_{ijkl} are functions of the reduced time ξ which is, in general, a nonlinear function of time because of Eq. (4). The E_{ijkl} are, therefore, nonlinear kernels in the set of integral equations, and the Laplace

transform and, hence, the elastic–viscoelastic correspondence principle cannot be applied. If the material properties are independent of time, i.e., in the present case, if the thermal field is independent of time, or if the material properties are independent of temperature, then the matrix elements E_{ijkl} in Eq. (32) are functions of $(t - t')$. Hence, we are then able to apply the Laplace transform to Eq. (32). If p is the transform variable and if the barred functions indicate transforms, we obtain

$$\{\bar{\mathbf{t}}_n\} = \int_{V_I} [\Phi^{-1}]^T [\psi]^T [p\bar{\mathbf{E}}] [\psi] [\Phi^{-1}] \, dV_I \{\bar{\mathbf{U}}\}$$
$$- \int_{V_I} [\Phi^{-1}]^T [\psi]^T [p\bar{\mathbf{E}}] \{\overline{\theta\alpha}\} \, dV_I$$
$$- \int_{V_I} [\Phi^{-1}]^T [\phi]^T \{\bar{\mathbf{f}}\} \, dV_I \qquad (33)$$

If we identify the elements $[p\bar{\mathbf{E}}]$ with the corresponding elastic moduli and the transformed quantities with the corresponding elastic quantities, Eq. (33) represents the formulation for the corresponding elastic problem, where the first volume integral on the right side of Eq. (33) represents the usual element stiffness matrix.

It follows that, given a linear elastic solution, the corresponding viscoelastic transformed solution for a particular p is obtained by substituting for the corresponding quantities the p-multiplied transformed viscoelastic moduli, $p\bar{E}_{ijkl}(p)$, the transformed product of the thermal field and the expansion coefficients, $\overline{\theta\alpha}(p)$, and the transformed body forces $\bar{f}_i(p)$, and by considering $\bar{t}_n(p)$ and $\bar{U}(p)$ as functions of p.

C. The Computer Program ELAS

A computer program that can be used in the studies described above must have some special features. It should reflect all possible capabilities offered by contemporary studies in the field of the finite element method. Factors that restrict the use of this method, such as excessive computing time, limited storage capacity of computers, and accumulation of round-off errors, must be minimized. These factors are not completely independent of each other, i.e., the computing time increases drastically by the use of out-of-core devices for the increase of the storage capacity, and the use of double-precision arithmetic to decrease the effects of round-off errors decreases the storage capacity and increases the computing time. Therefore, a computer program that will be used for these purposes must be as efficient as possible in using core memory space, shortening computing time, and reducing round-off errors. The computer program ELAS, developed in Ref. 18, has been prepared to achieve this goal. Its special features are summarized below:

(1) Types of structural problems that can be handled are frames, stretching and bending of plates and shells, two- and three-dimensional elastic solids, and axisymmetrical shells and solids.

(2) The dynamic memory allocation allows the use of adequate storage space for a given problem. This also provides access to a larger core memory capacity if larger-scale computers become available.

(3) An automatic relabeling procedure that minimizes the bandwidth of the stiffness matrix is incorporated.

(4) The boundary conditions are imposed at the time of assembly of the coefficient matrix. This eliminates unnecessary use of core memory by coefficients of equations to be eliminated later. Every type of displacement and force boundary condition that arises in practice can be imposed.

(5) For continuous structures, the stresses can be computed either as average values in the elements, or, by spending a little more computing time, they can be computed at the nodal points by using the best-fit strain tensor in this region.

(6) The structural material may be isotropic, orthotropic, or general anisotropic. It may be homogeneous or nonhomogeneous. The effects of temperature changes for all types of structures and the effects of temperature gradients for frames, plates, and shells can be computed. The body forces due to arbitrary constant acceleration fields can be considered.

(7) The capacity depends on the type and number of elements, the bandwidth of the stiffness matrix, and the number of unknowns that are being retained after the imposition of boundary conditions. For an average type of problem, 500–700 unknowns can be handled on the IBM 7094 (32K) Model I computer in less than 5 min.

The complete treatment of these features and the guide for using this program are presented in Ref. 18. Although this program, in its present form, is strictly for use in solving linearly elastic problems, during its development more general stress analysis problems have been anticipated. Its overall structure can easily be altered by the addition of subroutines; or the subroutines that have been developed for this program can be used with other driving main programs for different purposes.

Before any further development beyond linear elasticity, the use of ELAS, as it now stands, will help to understand and clarify many of the complex problems of solid propellant stress analysis. Further program developments into the area of linear and nonlinear viscoelasticity will then follow along lines indicated in the sections above.

V. Results of Linear Elastic Studies

In this section, some examples of linear elastic stress analysis for the cylindrical axisymmetrical motor grains and for the spherical motor grains are presented. The objectives are:

(1) To provide some explanation of the steps that lead to the complete analysis of a given case. The complete analysis covers the choice of the various models and the geometrical and physical idealizations of the chosen model, i.e., mesh topology and material properties, boundary conditions, loadings, the choice of regions of interest, the comparison and the interpretation of the results, and the improvement of the results, if necessary.

(2) To compare the results obtained here with those previously obtained by others in Refs. 23 and 24.

(3) To emphasize various factors that are involved in obtaining meaningful results and that can be chosen correctly only if the analyst uses his experience and judgment in each new case.

The numerical results in this report were obtained by using the computer program ELAS and some additional subroutines. The cases considered in these studies represent only a small portion of the different possible cases that can be studied. Other complex models with complex boundary conditions, loadings, and material properties, such as variable temperature changes, anisotropic materials, combined analysis of grains and casings, more complex casing shapes, etc., can be studied if necessary.

A. Nike-Zeus Booster Grain Stress Analysis

The analysis of stresses has been carried out in order to compare the results obtained in this analysis with the ones available in Ref. 23, in which the stresses were obtained from the force method program and the photoelastic method and compared favorably with each other.

One-tenth of the axisymmetrical cross section was considered, as shown in Fig. 2. The boundary conditions, which are a result of the idealization of the physical model, are such that the boundary between the segments is restrained in the tangential direction, but is free in the radial direction. The external pressure loading was chosen for the analysis in order to obtain results directly comparable with those in Ref. 23; the material constants were also the same as in Ref. 23. The inner and central regions were divided into finer meshes, since these are the regions where high stress concentrations occur.

Figure 3 illustrates the comparison of tangential stresses along the hoop region. This figure corresponds to Fig. 1 of Ref. 23. The results of this study show an almost perfectly symmetrical distribution of stresses with respect to the symmetry axis of this region. In Ref. 23, the corresponding stress values are unsymmetrical, a result that might be due to the idealization of the hoop region by an unsymmetrical configuration of the bars and panels. However, both results are relatively close to each other.

Figure 4 illustrates the comparison of radial and tangential stresses shown in Fig. 4 of Ref. 23. The agreement in both cases is very good.

For this analysis, the computer time spent was less than 4 min on the IBM 7094, Model I. The total number of unknowns and equations was 707. This large number of equations could be accommodated by ELAS because of the relatively small bandwidth of the stiffness coefficient matrix. As has been shown in Ref. 18, this bandwidth is a function of the mesh topology and the labeling of the nodes.

An analysis similar to the one above has been carried out with a coarser mesh and a smaller number of elements and nodes. The mesh is shown in Fig. 5. The size and location of the region with a refined mesh is the same as in the previous case. A comparison has been made only for the deflection, and the numerical results agreed remarkably well with the corresponding ones obtained above, although the coarse mesh results are, in general, somewhat lower.

B. Two- and Three-Dimensional Analysis of Spherical Motor

Three different models have been chosen: (1) an axisymmetrical model with truncated inner star vertices, (2) a three-dimensional longitudinal slice of a half star, and (3) a two-dimensional transverse section passing through the center of the sphere.

In each case the grain material had a relatively low modulus of elasticity, with Poisson's ratio equal to 0.45 or 0.4995. The loading consisted of pressure acting only at the inner surface. The outer casing was treated as an axisymmetrical membrane shell, a spherical membrane shell, or a truss element corresponding, respectively, to each of the cases cited above. Since the deformation of the grain without the supporting casing is of the order of 0.10 in. or more, the 0.015-in. distance between the casing and the grain along the unbonded region is assumed to vanish during the early phase of deformation, and the grain is assumed to be supported completely by the casing during loading. A more realistic but more cumbersome procedure (not considered here) would be to solve the problem in two steps: (1) determine the loading and the stresses for which the unbonded surfaces touch the membrane and (2) superimpose the effect of complementary loading on the results obtained in the first step. This approach could be of interest for some specific stress-analysis problems.

The boundary conditions are assumed to be such that the outer perimeter of the transverse section at the nozzle end is completely fixed, while the inner perimeter at the opposite end is fixed only in the radial direction.

1. Axisymmetrical model. The geometrical idealization and the mesh topology are shown in Fig. 6. Two series of results were obtained for two types of boundary conditions, with Young's modulus equal to 10,000 psi and Poisson's ratio equal to 0.45. The displacements of the inner boundary of a typical section passing through the center of the sphere and corresponding to the boundary conditions shown in Fig. 6 are plotted in Fig. 7. If the boundaries are released and only one restrained in the y direction is imposed at nodal point 9, which is a minimum of restraint necessary to provide static stability, the radial displacements remain almost constant, while the displacements in the y direction increase 4–5 times. The physical interpretation of the boundary conditions of Fig. 6 is equivalent to a ring stiffener at both ends of the case and a perfect bond between the case and the grain along the outer ring at the nozzle end. The value of the ring load which arises from this hypothetical bond is given in Fig. 7.

The same computations as those above have been made using a grain material with Poisson's ratio equal to 0.4995. The resulting displacements were approximately 2–3 times smaller than those above, which is to be expected because of the increased bulk rigidity in the latter case (Fig. 8). Another set of computations has been done to determine the effect of the rigidity of the casing. When the modulus of elasticity of the grain is being decreased, holding all other variables constant, the stresses in the grain approach a hydrostatic state, while the stresses in the casing increase considerably, as is to be expected. Figure 9 illustrates a comparison of the radial stresses along a transverse section for two different thicknesses of casing. The peak stresses clearly approach the hydrostatic pressure equal to that applied to the inner boundary.

2. Three-dimensional model. A longitudinal slice of 25° 42′ 51″ has been isolated and analyzed as substitute for the complete three-dimensional model. The model obtained has been divided into hexahedrons, and the mesh topology is shown in Fig. 10. The outer boundary of the model is encased in a steel membrane shell that is supposed to be perfectly bonded to the grain at the nodes. The inner boundary is free and subject to pressure. The two interfaces of the slice with the other portions of the motor are assumed to be free along the slicing plane, but restrained in the orthogonal direction. The boundary conditions at the nozzle and head ends are similar to those of the axisymmetrical model. Results have been computed for 600 psi internal pressure, using a modulus of elasticity of 1300 psi and a Poisson's ratio of 0.4995. The comparison of the stresses along the transverse plane and the displacements along the inner boundary and transverse plane with the results of the previous axisymmetrical case is given in Figs. 11 and 12, respectively. The plane section in the three-dimensional model was inclined less than 5 deg, but it was assumed that the comparisons were still valid. Remarkably good agreements were obtained in all points except at those that are close to singular points such as sharp corners.

3. Transverse section model. Two-dimensional analyses of a transverse section model have been carried out for two different mesh topologies. In both cases, it was assumed that the section was of unit thickness of an infinitely long cylinder having the star-shaped section of the spherical motor. This then corresponds to a plane strain problem, and no three-dimensional effects exist. The case and the grain are, therefore, more flexible than the true spherical model. In fact, the displacements were approximately twice as large, and qualitative observations show that the radial displacements along the radial line passing through the hoop region have a similar pattern to those obtained in the axisymmetrical model. Two sets of radial displacements, corresponding to the irregular mesh of Fig. 13 and the regular mesh of Fig. 14, respectively, are plotted in Fig. 15. The refinement of the

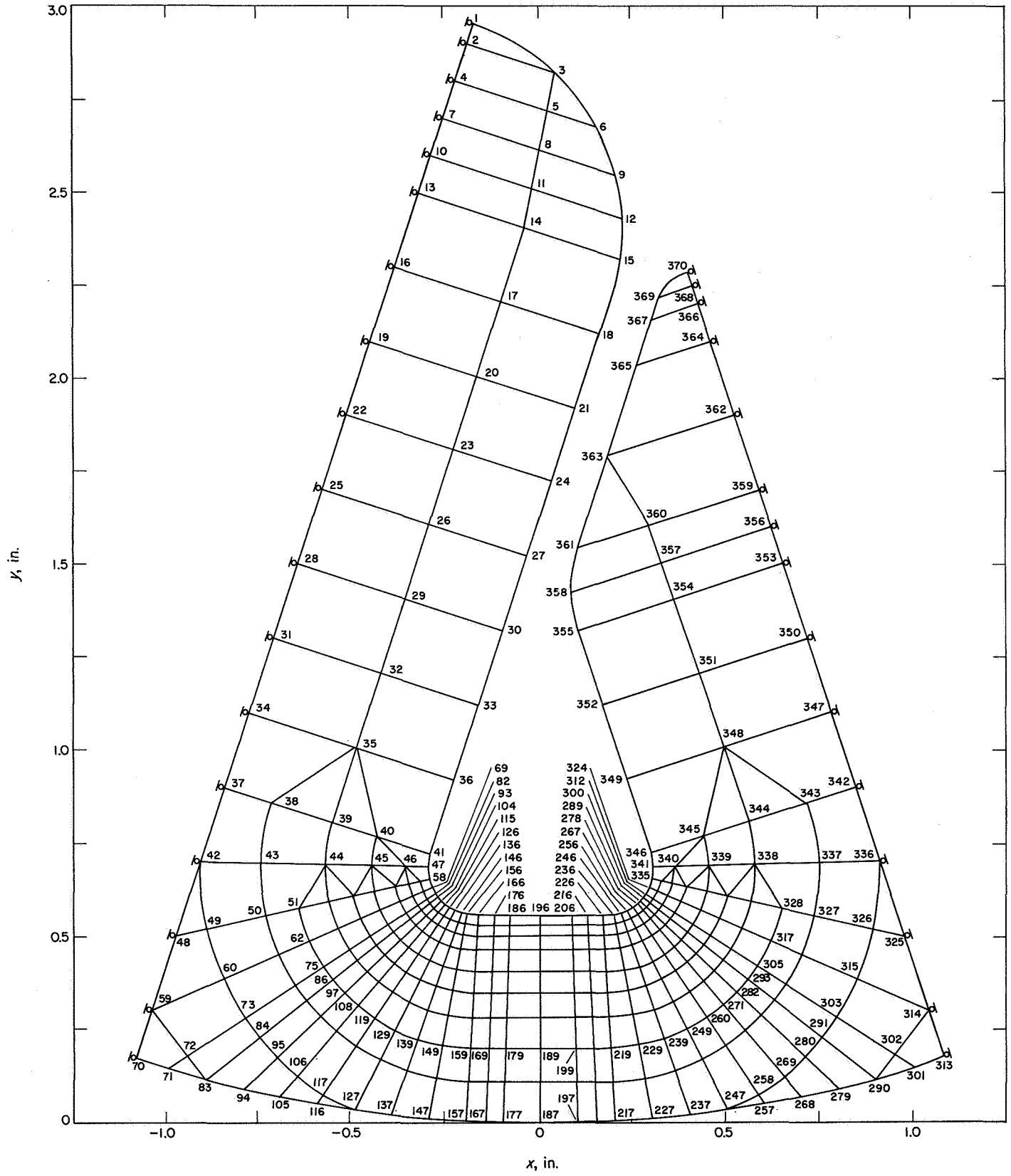

Fig. 2. Nike-Zeus booster finite element idealization

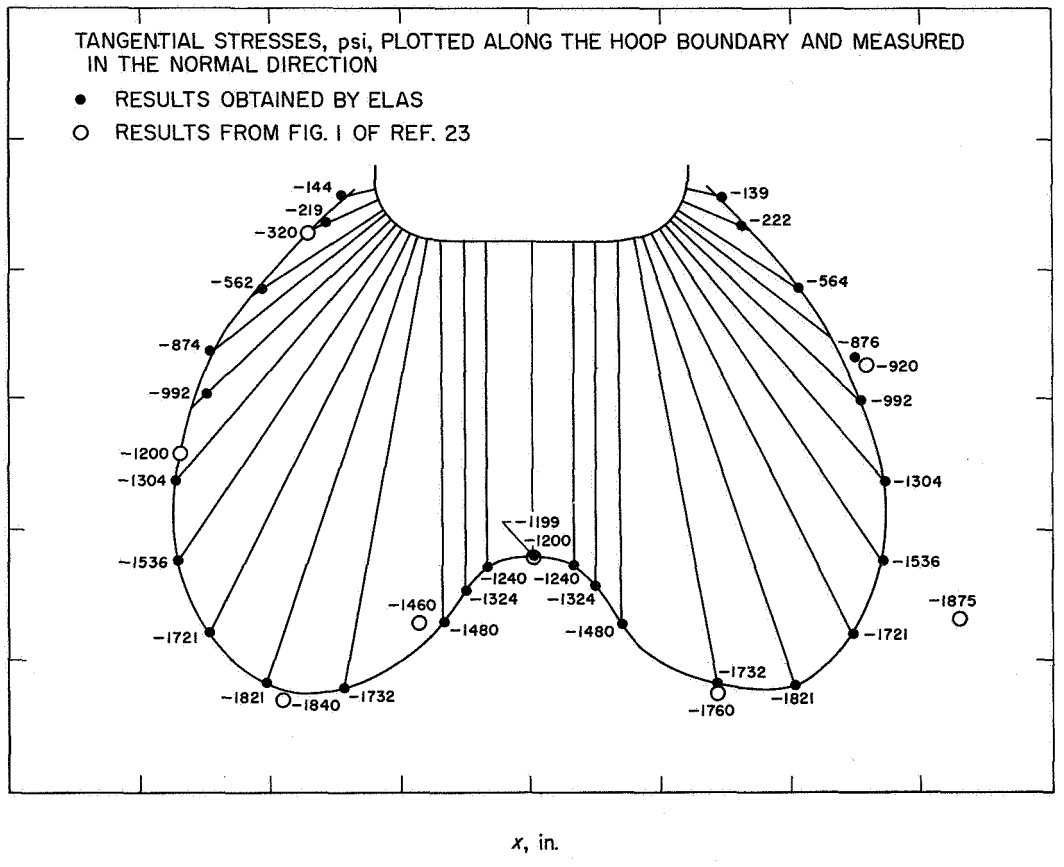

Fig. 3. Distribution of tangential stresses along the hoop region of the inner boundary

mesh (Fig. 14) results in an average increase of approximately 15% of the displacements.

The stresses along the same line have also been plotted in Fig. 14. For the irregular mesh the results are different from those obtained in the previous models and from those obtained for the regular mesh of this model. Qualitative and quantitative interpretation suggests that an irregular mesh can lead to erroneous results in the stress computations and should, therefore, be avoided.

Other computations with different values for the material constants were carried out in order to determine the contributions of round-off errors. For values of Poisson's ratio not close to 0.5, these effects were negligible for the problems considered here. The round-off errors are reflected in the computation of forces acting on the nodal points, i.e., the deviation of these forces from their true values is a measure of the effects of round-off errors. The use of the double-precision version of the subroutine for the solution of the equations decreases the effect of the round-off errors approximately 10 times. The effects on the final stress and displacement results are not appreciable. A double-precision assembly program for two-dimensional problems decreases the effects of round-off errors approximately 100 times. The effects on the final results are only a few percent.

Because the double-precision program has limitations of storage, for ELAS the storage locations for such computations do not exceed 10,000. For single-precision computations using ELAS, this number is more than 20,000. The conclusions of this study are that even with values of Poisson's ratio close to 0.5, the program can be used with confidence in its present form to obtain displacement results.

Another way of obtaining improved stress results is to isolate a small portion of interest from an entire region and analyze this portion as a separate problem. In this case the boundary conditions at the interface between the isolated portion and the remaining part will be the deflections of the nodal points from a coarse preceding analysis for the entire region.

During the course of this investigation, some additional subroutines were prepared for (1) the generation of the mesh topology and the coordinates corresponding to the axisymmetrical model and (2) the generation of the mesh topology corresponding to the transverse section analysis. With a few minor changes, these programs can be used for a number of other mesh topology configurations.

An important point that might be useful in the initial preparation of a problem is that the use of quadrilateral elements in two-dimensional, and hexahedral elements in three-dimensional, problems will considerably facilitate the use of the subroutines described above. Also, the final stress results are usually improved by the use of such elements.

VI. Conclusions

This report is a first step toward the development of capabilities for the stress analysis of solid propellant rocket motors consisting of thermoviscoelastic propellant grains and metal or composite material casings. It has been pointed out that the main difficulties at present in the determination of the stresses are associated with the lack of adequate computational techniques and with the fact that the constitutive properties of the materials are in many cases insufficiently known. This holds especially true for the prediction of the strength and failure properties of solid propellant grains.

The study of the elastic response of various grain configurations in the latter part of this report shows that even using the simplest form of constitutive equations, the analysis of stresses in solid propellant motors is a considerably complex problem. For more complex geometries, boundary conditions, loadings and material properties, correspondingly more computational efforts will have to be spent toward the determination of stress distributions in propellant grains. Critical areas in this respect are the preparation of input data and the interpretation of the numerical results. A general scheme for the automation of input operations and for the automated interpretation of the results in the form of graphical displays is, therefore, highly desirable.

The formulation of the linear viscoelastic problem indicates that only for rather special cases can the elastic–viscoelastic correspondence principle be applied, i.e., when the material properties are independent of thermal changes. Since the properties of almost all solid propellants are highly temperature-sensitive, it seems that the development of a program based on this principle is of considerably less value than the development of a program which does not utilize the correspondence principle, i.e., which solves a set of integral equations as pointed out in Section IV. Also, in view of possible extensions to nonlinear problem applications, the latter approach seems to be more attractive.

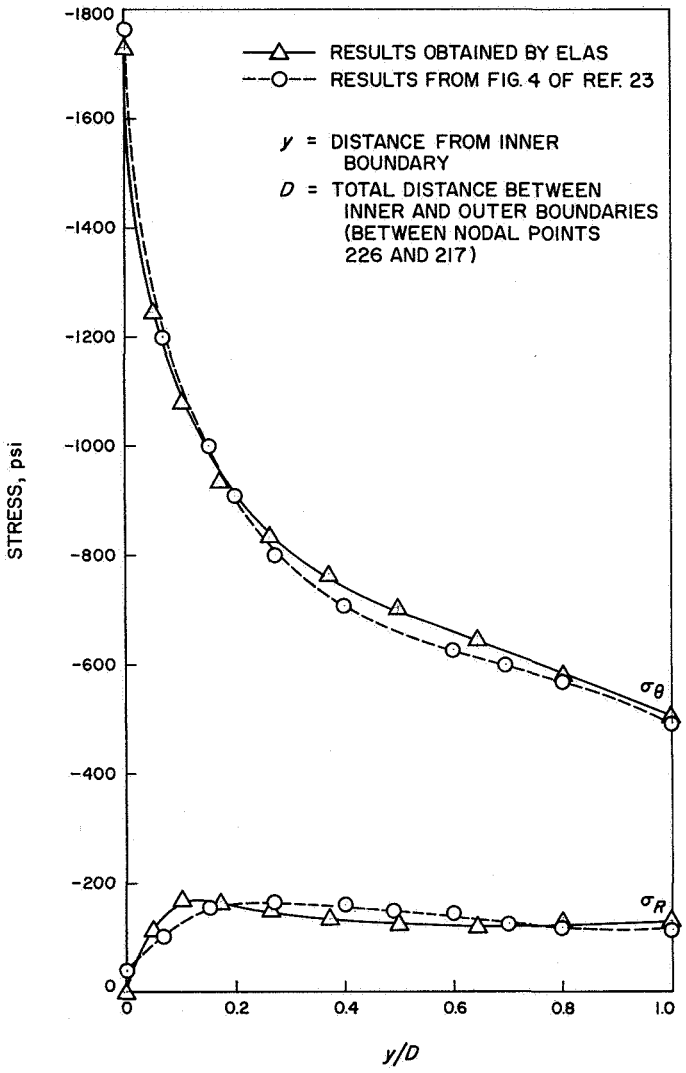

Fig. 4. Comparison of radial and tangential stresses along section through nodal points 217–226

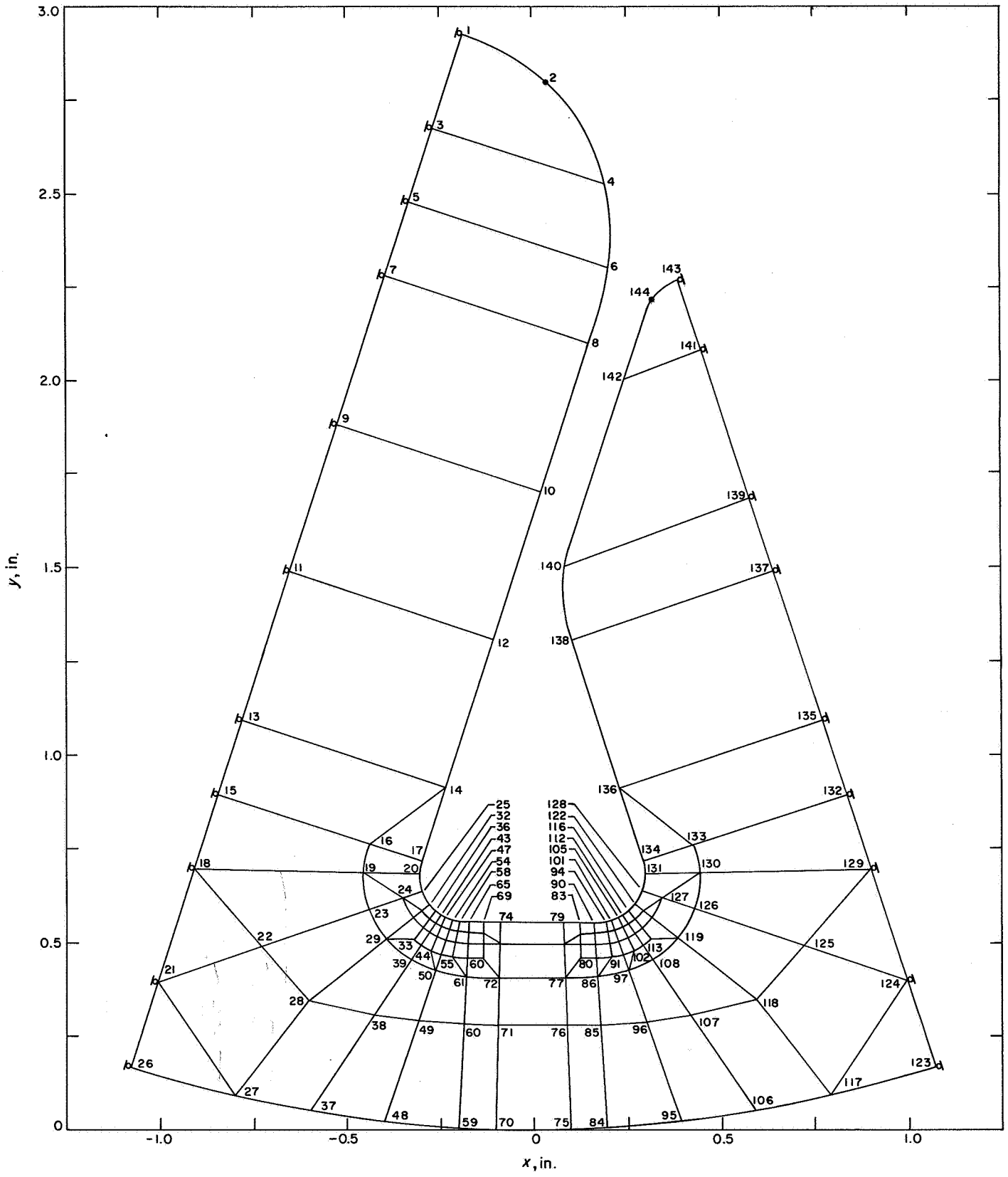

Fig. 5. Nike-Zeus booster finite element idealization; coarse mesh

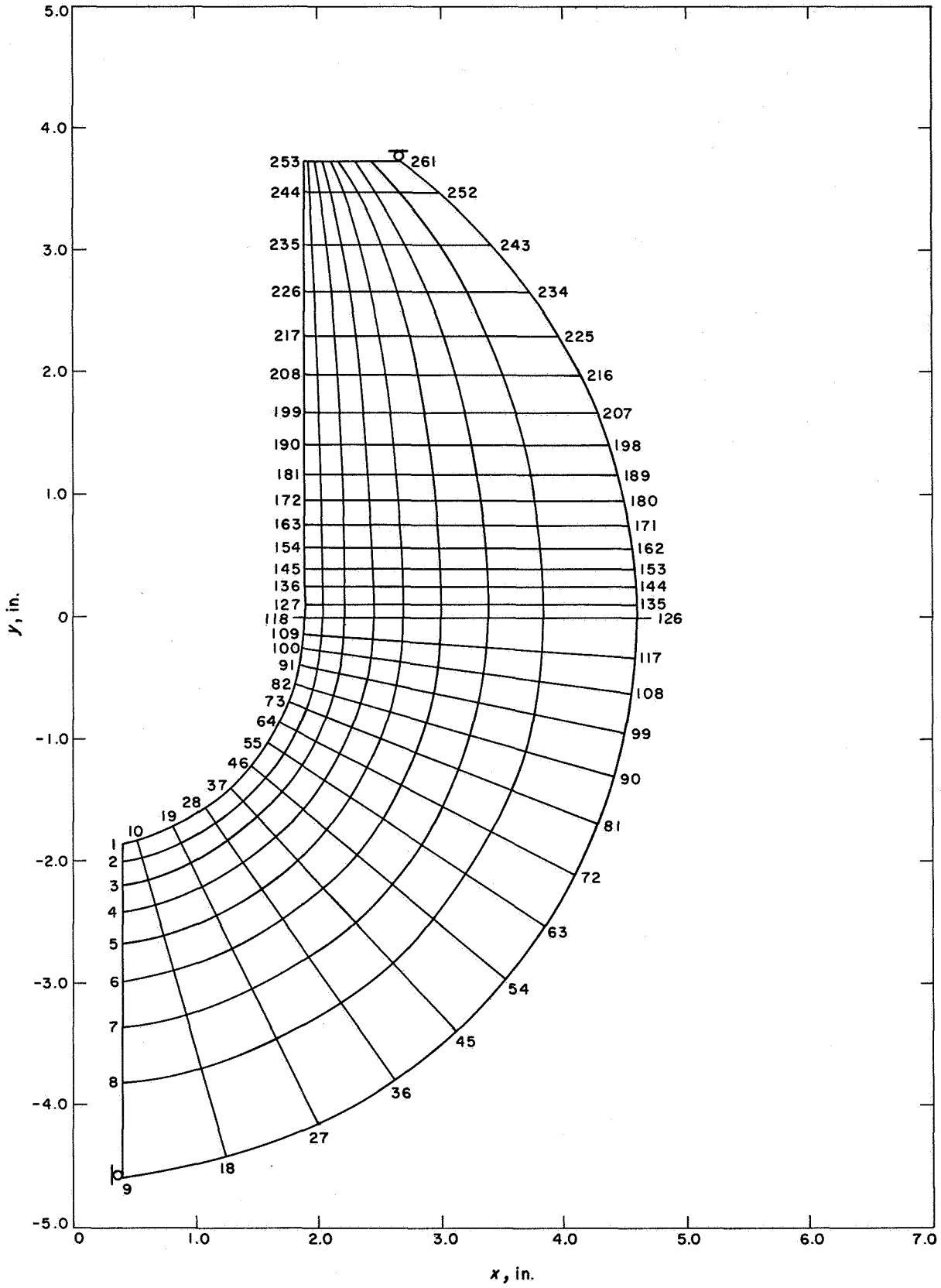

Fig. 6. Axisymmetrical model with regular boundary conditions

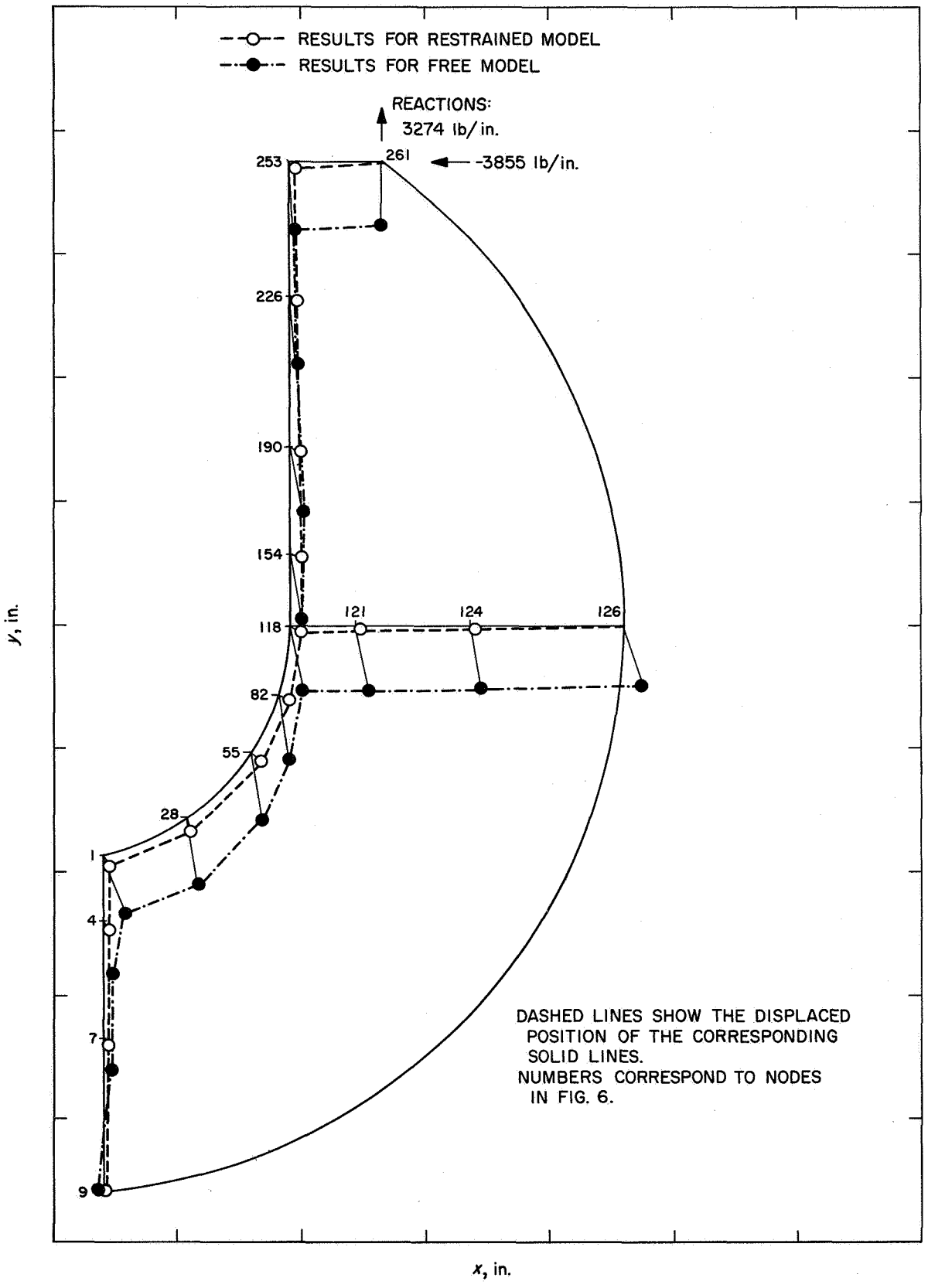

Fig. 7. Axisymmetrical model; effect of boundary conditions for Poisson's ratio $\nu = 0.45$

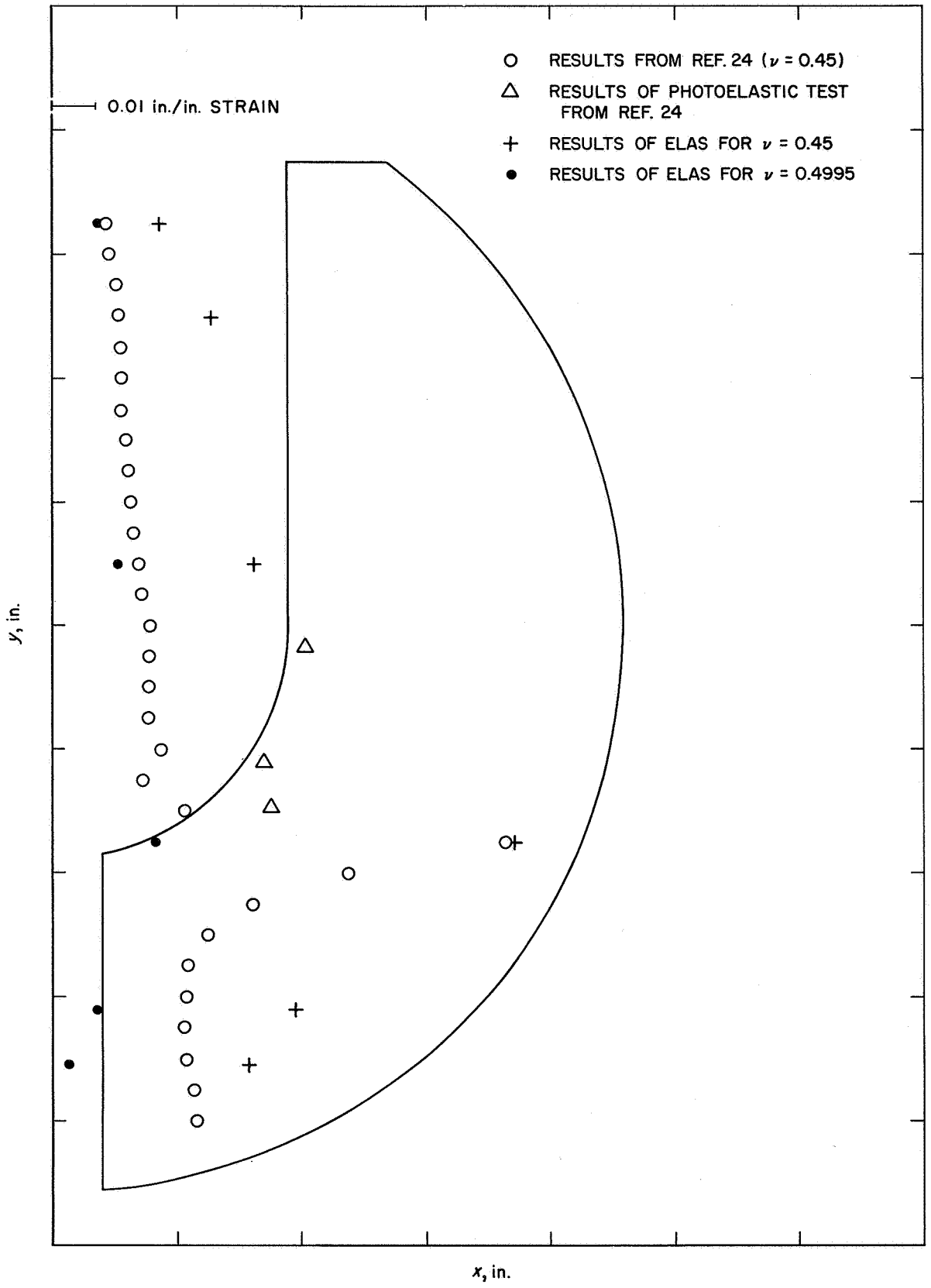

Fig. 8. Comparison of hoop strains ϵ_θ for different values of Poisson's ratio ν in axisymmetrical model

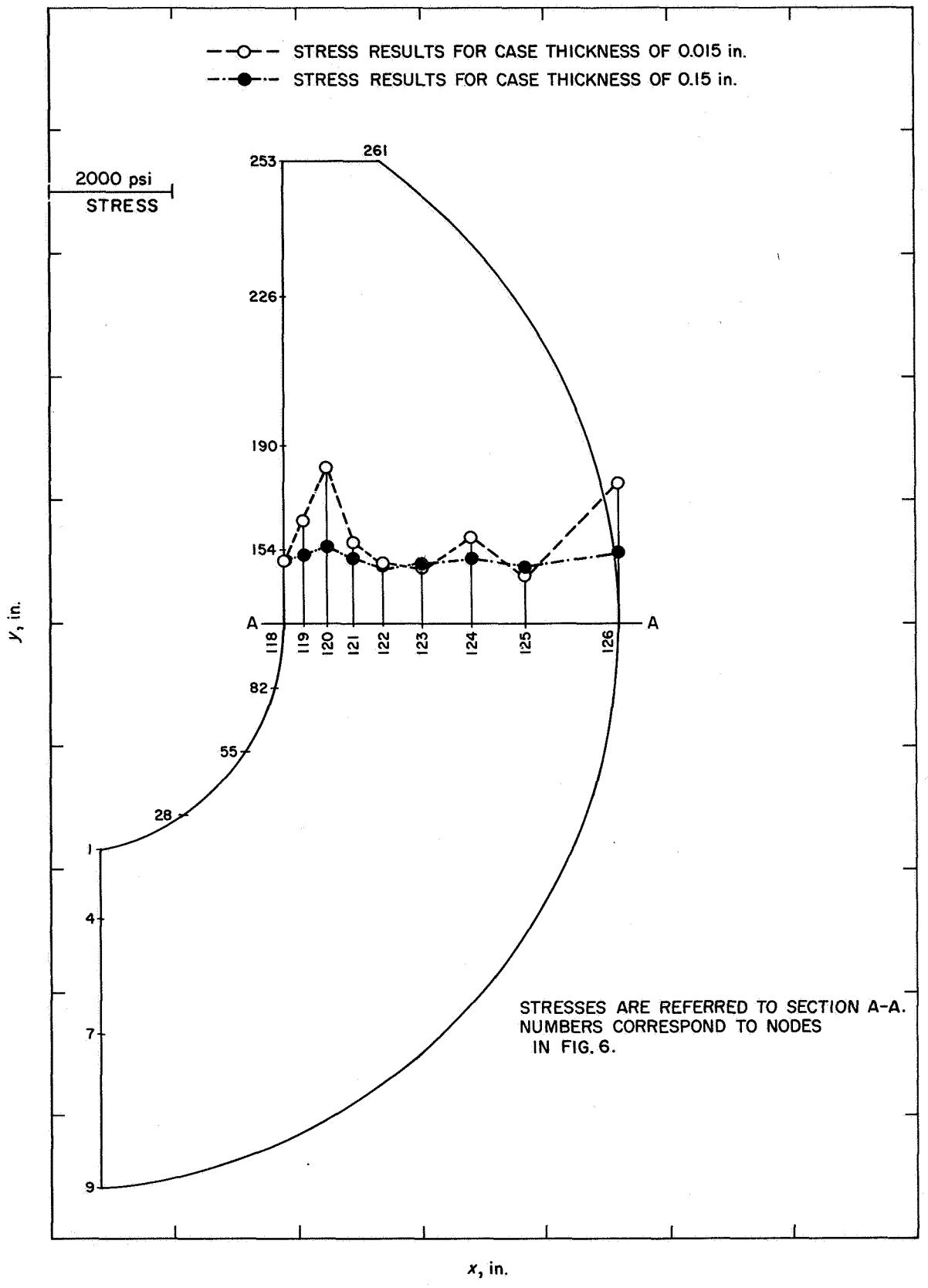

Fig. 9. Axisymmetrical model; effect of thickness of steel case on the radial stresses along section A-A

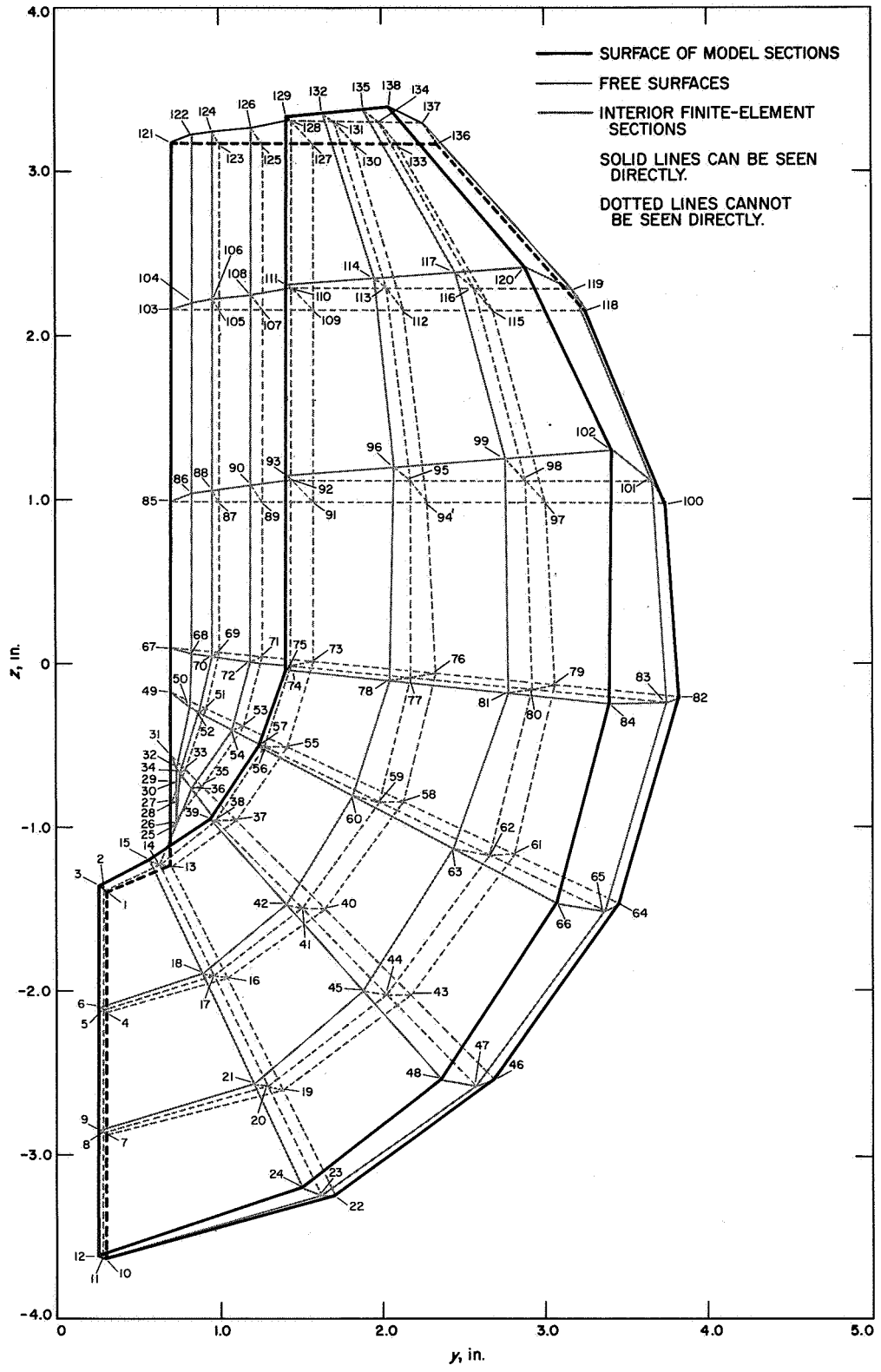

Fig. 10. Three-dimensional model; 25°42′51″ slice

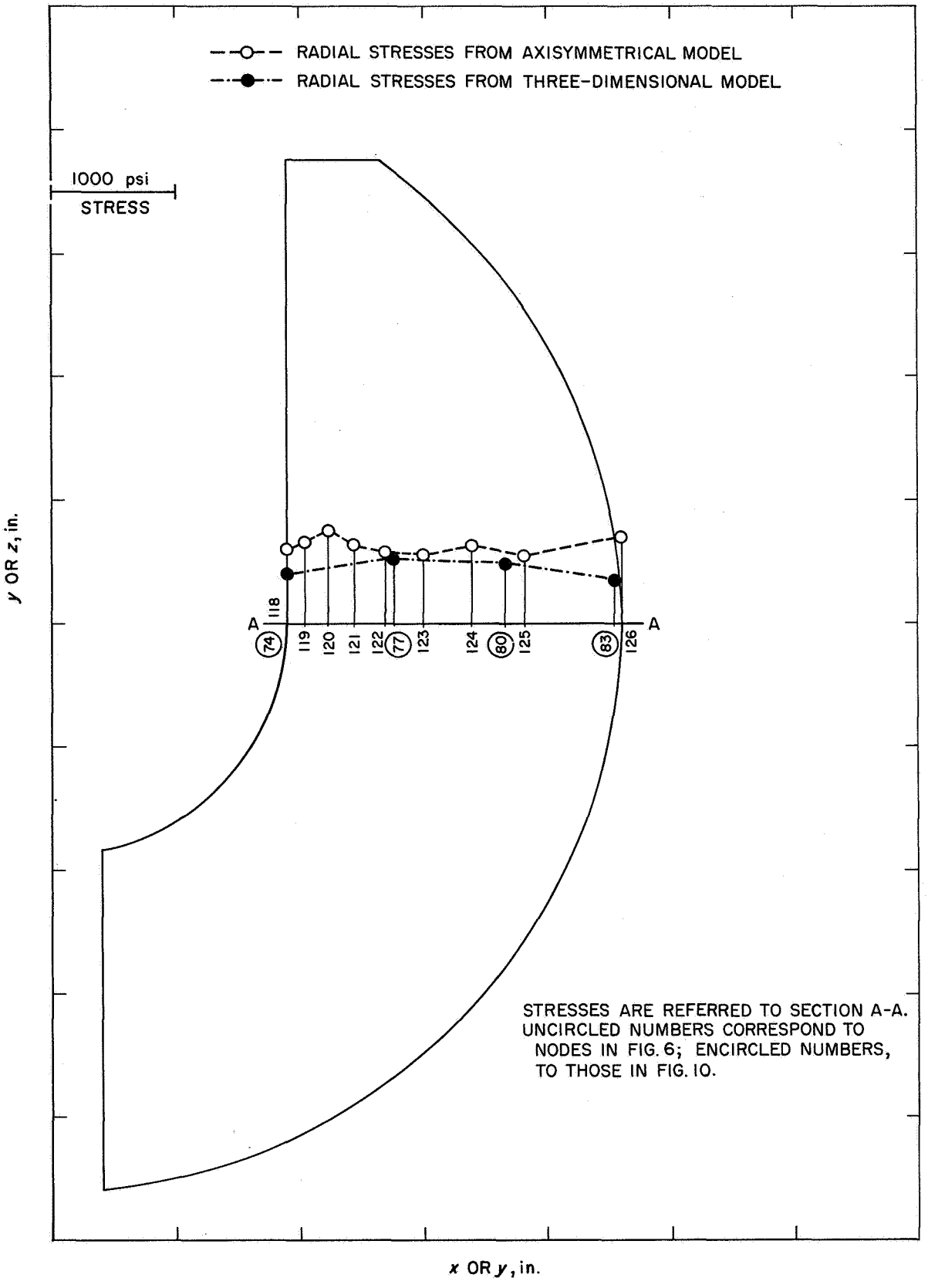

Fig. 11. Comparison of stresses for axisymmetrical and three-dimensional models

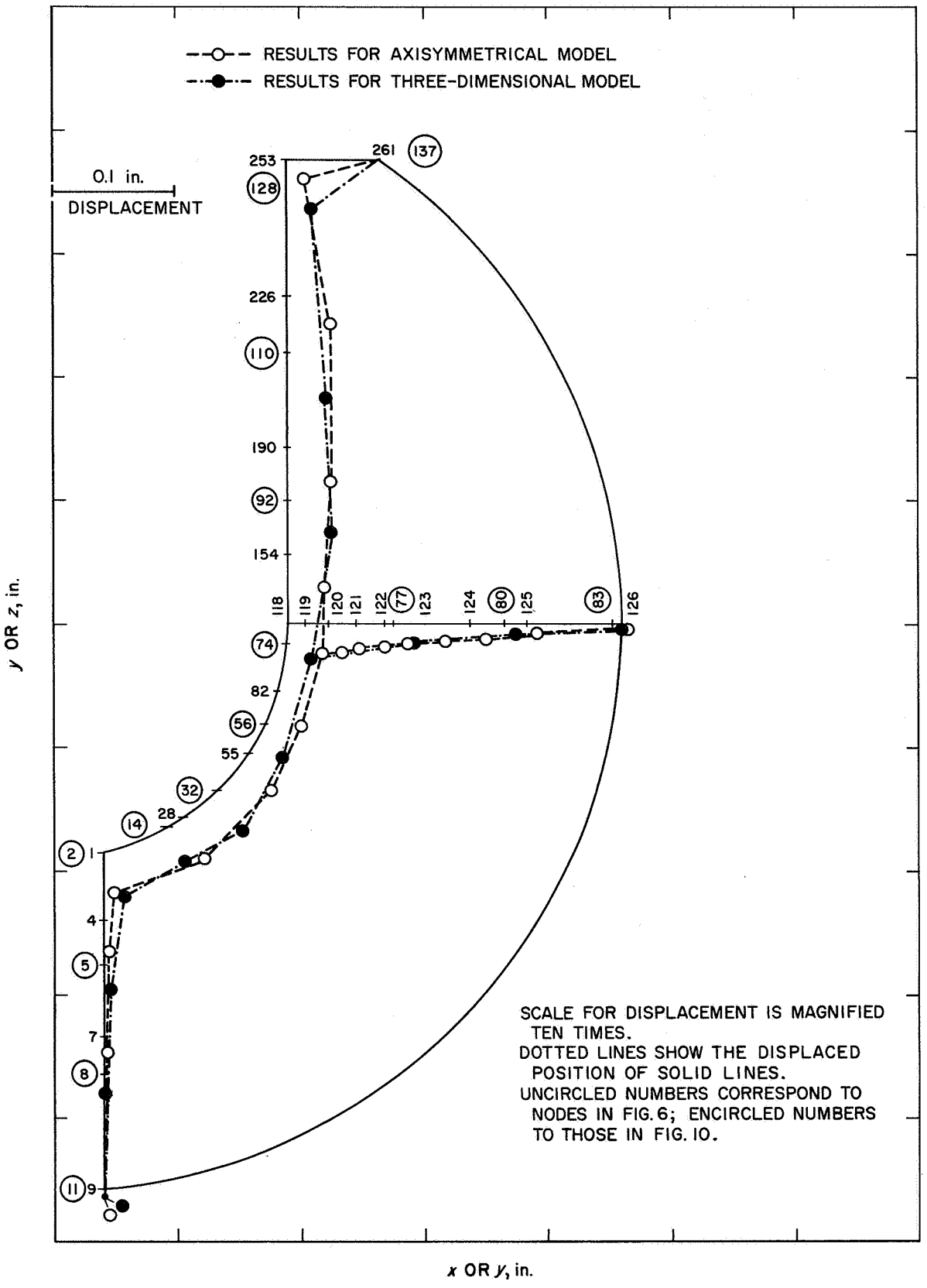

Fig. 12. Comparison of displacements for axisymmetrical and three-dimensional models

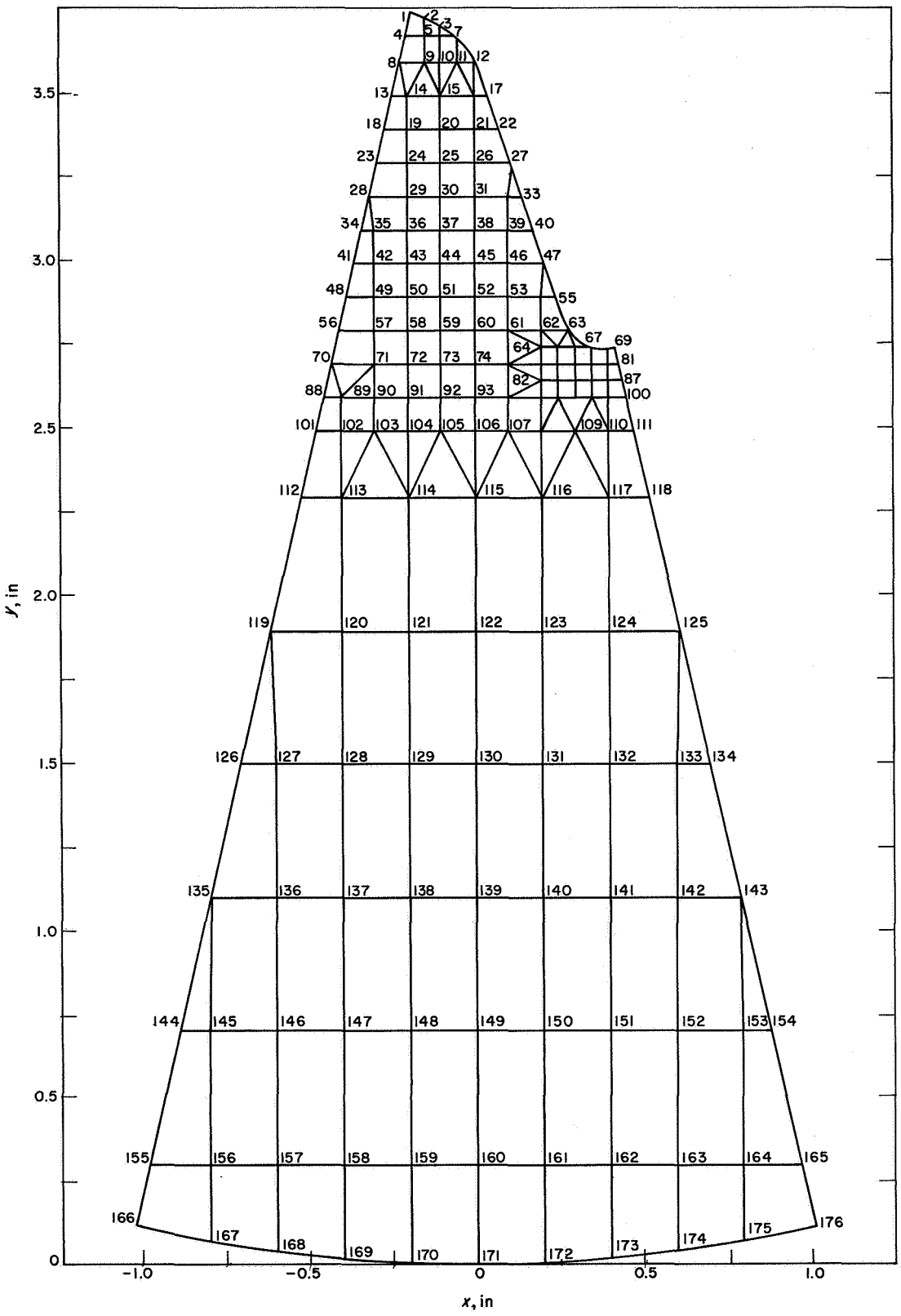

Fig. 13. Irregular mesh representation of the transverse section of the spherical motor

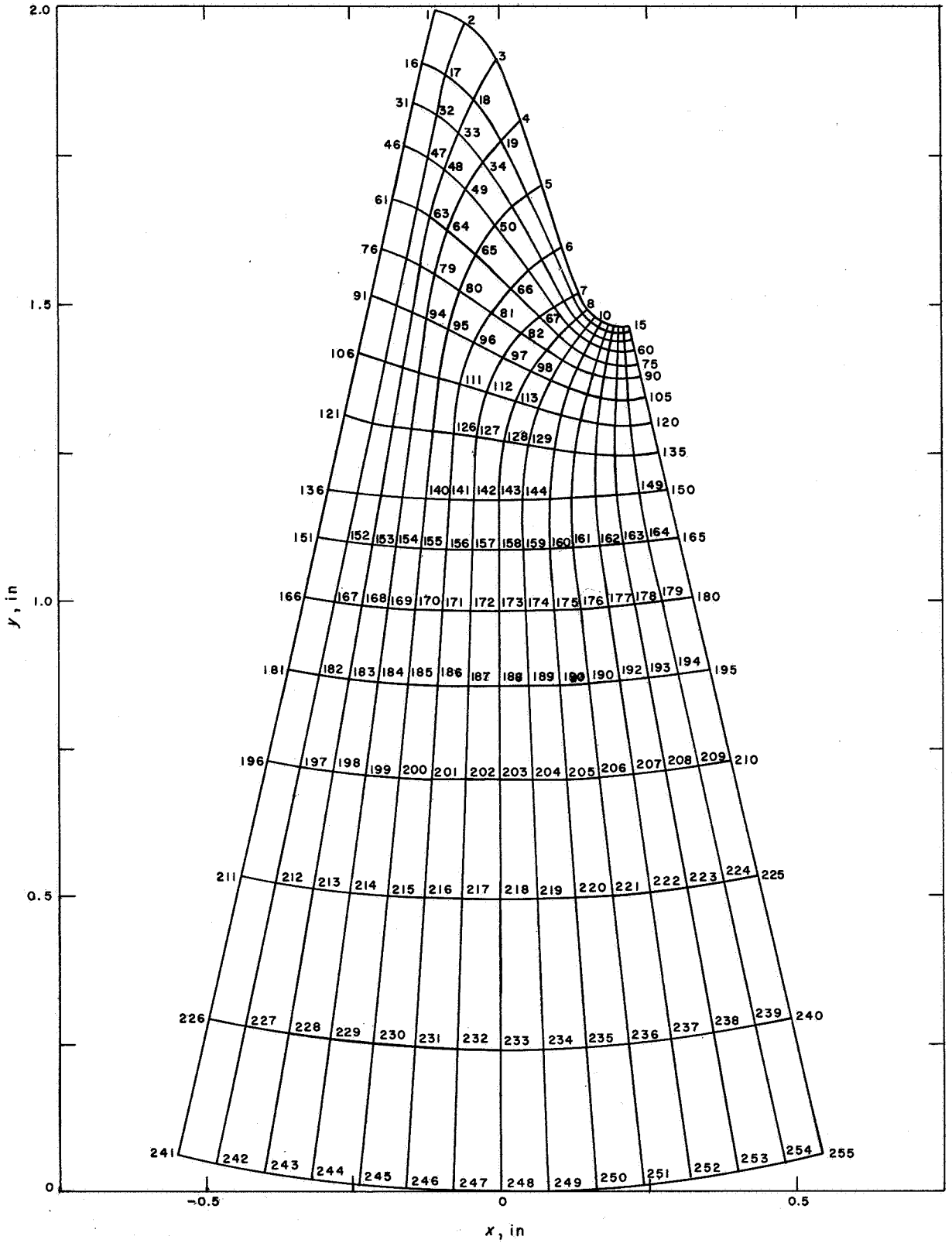

Fig. 14. Regular mesh representation of the transverse section of the spherical motor

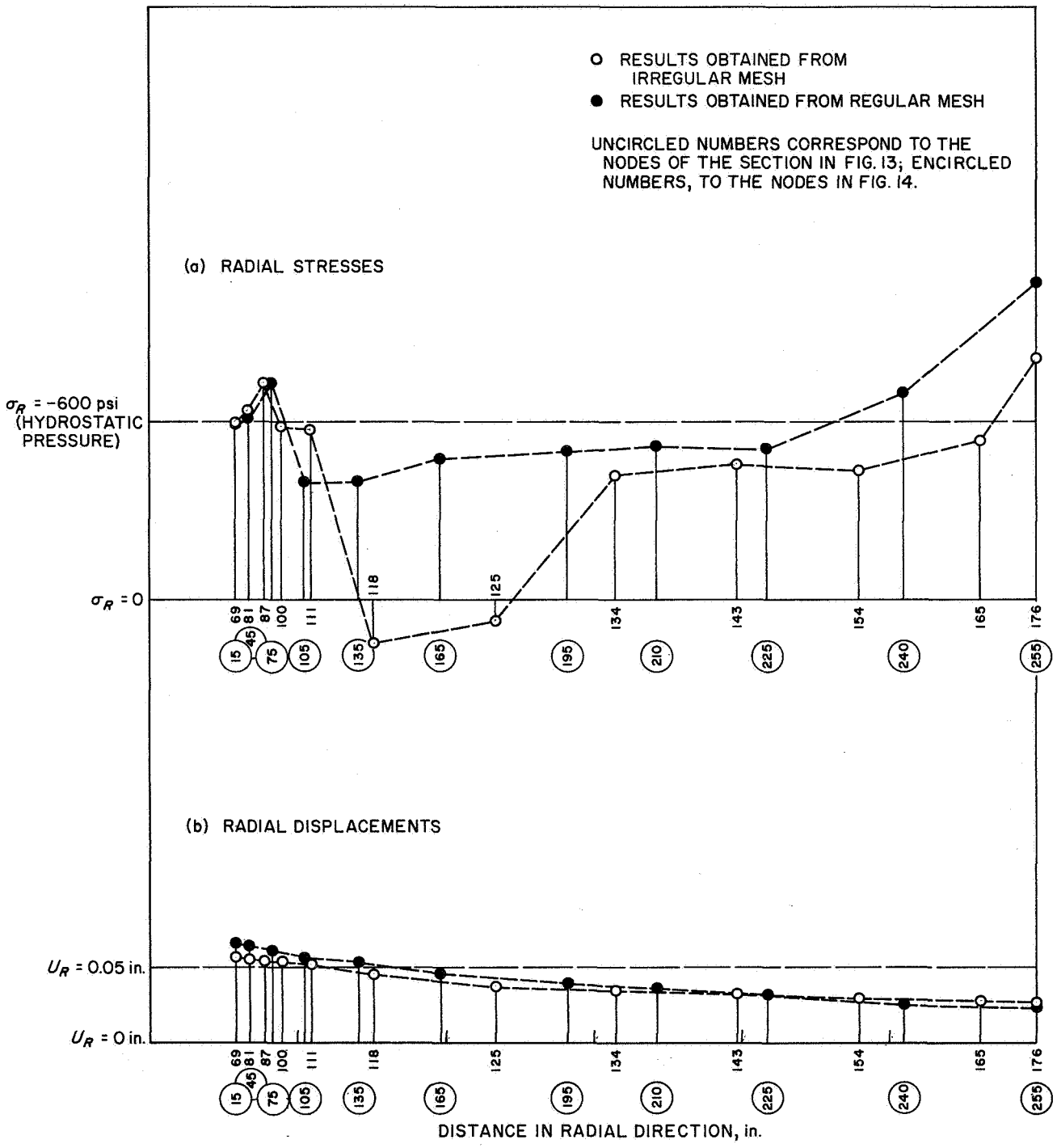

Fig. 15. Comparison of results obtained from irregular and regular meshes

References

1. Argyris, J. H., "Continua and Discontinua," in *Matrix Methods in Structural Mechanics*, AFFDL-TR-66-80, Proceedings of the Conference Held at Wright-Patterson Air Force Base, Oct. 26–28, 1965, sponsored by the Air Force Flight Dynamics Laboratory, Research and Technology Division, Air Force Systems Command, and the Air Force Institute of Technology Air University, Nov. 1966.

2. Zienkiewicz, O. C., and Cheung, Y. K., *The Finite Element Method in Structural and Continuum Mechanics*. McGraw-Hill Book Co., Inc., New York, 1967.

3. Taylor, R. L., and Chang, T. Y., "An Approximate Method for Thermoviscoelastic Stress Analysis," *Nuclear Engineering and Design*, Vol. 4, pp. 21–28, North Holland Publishing Co., Amsterdam, 1966.

4. Fitzgerald, J. E., "Analysis and Design of Solid Propellant Grains," in *Mechanics and Chemistry of Solid Propellants*, Proceedings of the 4th Symposium on Naval Structural Mechanics, Apr. 19–21, 1965. Edited by A. C. Eringen et al. Pergamon Press, 1967.

5. Biot, M. A., "Theory of Stress–Strain Relations in Anisotropic Viscoelasticity and Relaxation Phenomena," *J. Appl. Phys.*, Vol. 25, No. 11, pp. 1385–1391, Nov. 1954.

6. Biot, M. A., "Variational and Lagrangian Methods in Viscoelasticity," in *Deformation and Flow of Solids*, Proceedings of the IUTAM Colloquium, Madrid, 1955, pp. 251–263. Springer-Verlag, Berlin, 1956.

7. Biot, M. A., "Linear Thermodynamics and the Mechanics of Solids," in *Proceedings of the 3rd U.S. National Congress of Applied Mechanics*, pp. 1–18. American Society of Mechanical Engineers, 1958.

8. Schapery, R. A., "An Engineering Theory of Nonlinear Viscoelasticity With Applications," *Int. J. Solids Struct.*, Vol. 2, No. 3, pp. 407–415, July 1966.

9. Schapery, R. A., "Application of Thermodynamics to Thermomechanical Fracture and Birefringent Phenomena in Viscoelastic Media," *J. Appl. Phys.*, Vol. 35, No. 5, pp. 1451–1465, May 1964.

10. Schapery, R. A., "A Theory of Nonlinear Thermoviscoelasticity Based on Irreversible Thermodynamics," in *Proceedings of the 5th U.S. National Congress of Applied Mechanics*, pp. 511–530. American Society of Mechanical Engineers, 1966.

11. Staverman, A. J., and Schwarzl, F., "Linear Deformation Behavior of High Polymers," in *Die Physik der Hochpolymeren*, Vol. IV, Chapter 1. Edited by H. A. Stuart. Springer-Verlag, Berlin, 1956.

12. Morland, L. S., and Lee, E. H., "Stress Analysis for Linear Viscoelastic Materials With Temperature Variation," *Trans. Soc. Rheol.*, Vol. IV, pp. 223–263, 1960.

13. Alfrey, T., "Nonhomogeneous Stresses in Viscoelastic Media," *Quart. Appl. Math.*, No. 2, pp. 113–119, 1944.

References (contd)

14. Sternberg, E., "On Transient Thermal Stresses in Linear Viscoelasticity," in *Proceedings of the 3rd U.S. National Congress of Applied Mechanics*, pp. 673–683. American Society of Mechanical Engineers, 1958.

15. Muki, R., and Sternberg, E., "On Transient Thermal Stresses in Viscoelastic Materials With Temperature-Dependent Properties," *J. Appl. Mech.*, Vol. 18, pp. 193–207, June 1961.

16. Parr, C. H., "The Application of Numerical Methods to the Solution of Structural Integrity Problems of Solid Propellant Rockets," in *Solid Rocket Structural Integrity Abstracts*, Vol. 1, No. 2, p. 2-56, Oct. 1964.

17. Melosh, R. J., and Christiansen, H. N., *Structural Analysis and Matrix Interpretive System (SAMIS) Program: Technical Report*, TM 33-311. Jet Propulsion Laboratory, Pasadena, Calif., Nov. 1, 1966.

18. Utku, S., and Akyuz, F. A., *ELAS—A General-Purpose Computer Program for the Equilibrium Problems of Linear Structures: Vol. I, User's Manual*, TR 32-1240. Jet Propulsion Laboratory, Pasadena, Calif., Feb. 1, 1966. Also *Vol. II, Documentation*, in preparation.

19. Green, A. E., and Zerna, W., *Theoretical Elasticity*. Oxford University Press, New York, 1954.

20. Ferry, J. D., *Viscoelastic Properties of Polymers*, Chapter 4. John Wiley and Sons, Inc., New York, 1961.

21. Halpin, J. C., and Polley, H. W., "Observations on the Fracture of Viscoelastic Bodies," *J. Composite Mater.*, Vol. 1, p. 64, 1967.

22. Knauss, W. G., "An Upper Bound on Failure in Viscoelastic Materials Subjected to Multiaxial Stress States," in *Mechanical Behavior Working Group, 6th Meeting*, CPIA Publication 158, Vol. 1. Publication of a meeting held at the Jet Propulsion Laboratory, Pasadena, Calif., Dec. 5–6, 1967. Compiled and edited by the Chemical Propulsion Information Agency, Silver Spring, Maryland, Oct. 1967.

23. Frick, R. D., and Gilbertson, A. O., *Analysis of Nike-Zeus Booster Grain Model by Redundant Force Method and Comparison to Photoelastic Study*, Report SM-43926. Missile & Space Systems Division, Douglas Aircraft Company, Santa Monica, Calif., Aug. 1963.

24. Melette, R. V., et al., *A Grain Structural Analysis on a Spherical Motor*, Report SM-52244. Missile & Space Systems Division, Douglas Aircraft Company, Santa Monica, Calif., Feb. 1966.